

CTCF regulates cell cycle progression of $\alpha\beta$ T cells in the thymus

Helen Heath^{1,6,7}, Claudia Ribeiro de Almeida^{2,3,7}, Frank Sleutels¹, Gemma Dingjan², Suzanne van de Nobelen¹, Iris Jonkers⁴, Kam-Wing Ling², Joost Gribnau⁴, Rainer Renkawitz⁵, Frank Grosveld¹, Rudi W Hendriks^{2,3,*} and Niels Galjart^{1,*}

¹Department of Cell Biology and Genetics, Erasmus MC, Rotterdam, The Netherlands, ²Department of Immunology, Erasmus MC, Rotterdam, The Netherlands, ³Department of Pulmonary Medicine, Erasmus MC, Rotterdam, The Netherlands, ⁴Department of Reproduction and Development, Erasmus MC, Rotterdam, The Netherlands and ⁵Institute for Genetics, Justus-Liebig-Universitaet Giessen, Giessen, Germany

The 11-zinc finger protein CCCTC-binding factor (CTCF) is a highly conserved protein, involved in imprinting, long-range chromatin interactions and transcription. To investigate its function *in vivo*, we generated mice with a conditional *Ctcf* knockout allele. Consistent with a previous report, we find that ubiquitous ablation of the *Ctcf* gene results in early embryonic lethality. Tissue-specific inactivation of CTCF in thymocytes specifically hampers the differentiation of $\alpha\beta$ T cells and causes accumulation of late double-negative and immature single-positive cells in the thymus of mice. These cells are normally large and actively cycling, and contain elevated amounts of CTCF. In *Ctcf* knockout animals, however, these cells are small and blocked in the cell cycle due to increased expression of the cyclin-CDK inhibitors p21 and p27. Taken together, our results show that CTCF is required in a dose-dependent manner and is involved in cell cycle progression of $\alpha\beta$ T cells in the thymus. We propose that CTCF positively regulates cell growth in rapidly dividing thymocytes so that appropriate number of cells are generated before positive and negative selection in the thymus.

The EMBO Journal (2008) 27, 2839–2850. doi:10.1038/emboj.2008.214; Published online 16 October 2008

Subject Categories: immunology; chromatin & transcription
Keywords: cell cycle; chromatin; CTCF; nuclear organization; T cells

*Corresponding authors. N Galjart, Department of Cell Biology and Genetics, Erasmus MC Rotterdam, PO Box 2040, 3000 CA Rotterdam, The Netherlands. Tel.: +31 10 7043163; Fax: +31 10 7044743; E-mail: n.galjart@erasmusmc.nl or RW Hendriks, Department of Pulmonary Medicine, Erasmus MC Rotterdam, PO Box 2040, 3000 CA Rotterdam, The Netherlands. Tel.: +31 10 7043700; Fax: +31 10 7044728; E-mail: r.hendriks@erasmusmc.nl

⁶Present address: Developmental Signalling Laboratory, London Research Institute, Lincoln's Inn Fields Laboratories, 44 Lincoln's Inn Fields, London WC2A 3PX, UK

⁷These authors contributed equally to this work

Received: 5 May 2008; accepted: 19 September 2008; published online: 16 October 2008

Introduction

The 11-zinc finger protein CCCTC-binding factor (CTCF) is a widely expressed and highly conserved transcriptional regulator implicated in many important processes in the nucleus (for reviews, see Ohlsson *et al*, 2001; Lewis and Murrell, 2004). In line with this view, murine CTCF is essential for early embryonic development (Fedoriw *et al*, 2004). CTCF is the archetypal vertebrate protein that binds insulator sequences, DNA elements that have the ability to protect a gene from outside influences (Bell *et al*, 1999). Its methylation-sensitive interaction with the imprinting control region of the H19/insulin-like growth factor 2 (*Igf2*) genes indeed controls enhancer access (Bell and Felsenfeld, 2000; Hark *et al*, 2000; Fedoriw *et al*, 2004). CTCF-mediated insulator activity has been predicted at several other sites including the *DM1* locus and boundaries of domains that escape X-chromosome inactivation (Filippova *et al*, 2001, 2005). We have shown that CTCF mediates long-range chromatin interactions and regulates local histone modifications in the β -globin locus (Splinter *et al*, 2006). Evidence has furthermore been presented for a function of CTCF in inter-chromosomal interactions between *Igf2* and other loci (Ling *et al*, 2006). During mitosis, CTCF remains bound to mitotic chromosomes, possibly facilitating reformation of higher-order chromatin loops after mitosis (Burke *et al*, 2005). Taken together, these data suggest that CTCF is an essential organizer of imprinting, long-range chromatin interactions and transcription.

Genome-wide mapping of CTCF-binding sites revealed ~14 000 sites, whose distribution correlates with genes but not with transcriptional start sites (Kim *et al*, 2007). Strikingly, the 20-bp consensus motif found in the majority of the sites is virtually identical to a consensus sequence (called LM2*), which is bound by CTCF and is found in ~15 000 conserved non-coding elements (CNEs) in the human genome (Xie *et al*, 2007). Thus, CTCF-binding sites are part of CNEs, which are conserved across species and appear to have regulatory functions. High-resolution profiling of histone methylation in the human genome showed that CTCF sites mark boundaries of histone methylation domains (Barski *et al*, 2007) consistent with a function of CTCF as an insulator protein. Genome-wide analyses also revealed CTCF-binding sites near genes displaying extensive alternative promoter usage, including *Protocadherin* γ , the *Immunoglobulin (IG) λ light chain* and the *T cell receptor (TCR) α/δ and β chain* loci. In mice, CTCF-dependent insulators were found downstream of the *Tcr α/δ* and the *Ig heavy chain* loci (Magdinier *et al*, 2004; Garrett *et al*, 2005). Moreover, in T cells, CTCF-binding sites overlap significantly with DNase I hypersensitive sites (HS), suggesting that CTCF is somehow involved in global T-cell gene expression (Boyle *et al*, 2008). These data imply an important function of CTCF in lymphocytes, in particular in the regulation of gene transcription and recombination targeting in complex loci.

T-cell progenitors differentiate in the thymus, where early precursors (lacking the cell surface markers CD4 and CD8 and therefore termed double-negative (DN) cells) develop into mature CD4 or CD8 single-positive (SP) T cells, following a regulated differentiation programme (see Supplementary Figure S1 for a schematic overview; for review, see Rothenberg and Taghon, 2005). The DN precursor population is generally subdivided into four distinct developmental stages (DN1–DN4), which are defined by differential expression of the cell surface markers CD25 and CD44 (interleukin-2 receptor and phagocyte glycoprotein 1, respectively). Further differentiation of T cells depends on rearrangement of the *TCR* gene segments of four loci, that is, α , β , γ and δ . Most mature T cells express an $\alpha\beta$ TCR on their cell surface. These are the T cells involved in the classic adaptive immune response. $\gamma\delta$ T cells represent only a small fraction of T cells in lymphoid organs of humans and mice (1–5%) and line the epithelial layer of various organs, including the small intestine, but their function remains somewhat enigmatic (for review, see Chien and Konigshofer, 2007). The choice of whether the α and β *TCR* genes are rearranged, or the γ and δ genes, is made at the DN2–DN3 stage in the thymus.

TCR β gene rearrangement is initiated and completed at the DN3 stage. Upon productive (in-frame) rearrangement of the *TCR* β gene, the *TCR* β chain associates with the invariant pT α chain on the cell surface and forms the pre-TCR complex. Cells that have passed this so-called ‘ β -selection’ checkpoint are termed ‘ β -selected’ cells. The pre-TCR complex signals cells to proliferate and to downregulate CD25 expression. Cells subsequently acquire both CD4 and CD8 coreceptors to become double-positive (DP) cells, with CD8 usually being expressed first in most mouse strains (immature SP (ISP) cells). As a result, the late DN3, DN4 and ISP stages consist of large cycling cells (see Supplementary Figure S1). The DP cells then leave the cell cycle and rearrange their *TCR* α gene locus. If *TCR* α gene recombination is productive, *TCR* $\alpha\beta$ is expressed on the cell surface of DP cells. *TCR* $\alpha\beta$ -bearing immature cells are selected for major histocompatibility complex (MHC) recognition during the process of positive selection. *TCR* $\alpha\beta$ receptors with specificity for MHC class I will develop into the CD8-positive (CD8⁺) T-cell lineage, whereas receptors recognizing MHC class II will become CD4-positive (CD4⁺) T cells. DP thymocytes that fail to recognize MHC class molecules die ‘by neglect’, whereas potential self-reactive T lymphocytes are eliminated by a process called negative selection. When combined, these selection processes result in the generation of CD4 and CD8 SP thymocytes with *TCR* $\alpha\beta$ receptors that can recognize non-self-antigens presented by MHC class II and I proteins, respectively. Mature SP cells exit the thymus and circulate to the periphery as naive CD4⁺ and CD8⁺ T cells.

To circumvent the problem of embryonic lethality (Fedoriw *et al*, 2004), we generated mice with a conditional *Ctcf* allele (*Ctcf*^{fl/fl}). We examined the potential function of CTCF in *Tcr* gene rearrangement and global T-cell gene expression by deleting *Ctcf*^{fl/fl} in thymocytes. Here, we show that CTCF exerts an effect as a critical regulator of cell growth and proliferation following β -selection in the thymus. We demonstrate that CTCF expression varies during normal T-cell differentiation, with the highest levels occurring in subpopulations of relatively large and cycling thymocytes, including ISP cells. Interestingly, knockout of *Ctcf* results in a cell cycle

arrest at the ISP cell stage, owing to highly increased amounts of the cyclin-CDK inhibitors p21 and p27. CTCF-deleted DN4 and ISP cells are also significantly smaller than normal cells. We therefore propose a global function of CTCF as a positive regulator of cell growth in $\alpha\beta$ T cells.

Results

Conditional deletion of the *Ctcf* gene in developing T lymphocytes

To understand CTCF function *in vivo*, we generated a conditional *Ctcf* allele (*Ctcf*^f) by inserting *loxP* sites upstream of exon 3 and downstream of exon 12 (Figure 1A). Equivalent levels of CTCF are expressed in *Ctcf*^{fl/fl} and wild-type mice (data not shown). *Ctcf*^{+/fl} mice were crossed with mice expressing Cre recombinase ubiquitously (Sakai and Miyazaki, 1997). This causes removal of *Ctcf* exons 3–12 from *Ctcf*^f, yielding the *Ctcf*⁻ allele, in which a *Ctcf*-*lacZ* fusion transcript is expressed instead of *Ctcf* (Figure 1A). *Ctcf*^{+/-} mice appear normal and are fertile, but no homozygous knockouts are born from *Ctcf*^{+/-} crosses (Table I), consistent with an essential function of CTCF in early development (Fedoriw *et al*, 2004). Surprisingly, the ratio of wild-type to *Ctcf*^{+/-} littermates is higher than expected on a Mendelian basis in crosses among *Ctcf*^{+/-} mice and between wild-type and *Ctcf*^{+/-} mice (Table I). These data suggest that CTCF is required in a dose-dependent manner.

To obtain a T-cell-specific deletion of the *Ctcf* gene, we crossed *Ctcf*^{fl/fl} mice with *Lck-Cre* transgenic mice, in which the proximal *Lck* promoter drives expression of the Cre recombinase (Lee *et al*, 2001; Wolfer *et al*, 2002). Southern blot analysis shows almost complete deletion of the *Ctcf* gene in thymus, whereas in spleen, deletion is not evident (Figure 1B). These data reflect the specificity of the *Lck-Cre* transgene; they also indicate that *Ctcf* knockout T cells do not populate the spleen in large numbers. To evaluate the onset of *Ctcf*^f gene deletion, we analysed *lacZ* expression in thymocytes by flow cytometry using fluorescein-di- β -D-galactopyranoside (FDG) as a substrate in conjunction with cell surface markers that define thymocyte subpopulations. We find that deletion is almost complete from the DN2 stage onwards (Figure 1D). Western blotting shows that in thymic nuclear extracts from *Lck-Cre Ctcf*^{fl/fl} mice, CTCF protein levels are reduced to ~8% of control (Figure 1C). We conclude that ablation of the *Ctcf* gene results in an efficient depletion of the protein *in vivo*.

Defective *TCR* $\alpha\beta$ lineage development in *Lck-Cre Ctcf*^{fl/fl} mice

To examine the effects of a *Ctcf* deletion, thymocyte subpopulations in 6- to 8-week-old mice were analysed by flow cytometry. This revealed that *Lck-Cre Ctcf*^{fl/fl} mice have a reduced thymic cellularity (Table II). Whereas a specific defect is observed in $\alpha\beta$ T-cell development (Figure 2), $\gamma\delta$ T cells are not affected by *Ctcf* deletion (Supplementary data and Supplementary Figure S2), similar to what has been reported for conditional deletion of DNMT1 (Lee *et al*, 2001) and the RNaseIII enzyme Dicer (Cobb *et al*, 2006). Apparently, cell division, chromatin organization and gene regulation in $\gamma\delta$ T cells is quite different from $\alpha\beta$ T cells.

In $\alpha\beta$ T cells of *Lck-Cre Ctcf*^{fl/fl} mice, a decrease in the proportion and number of DP and SP cells, and a concomitant

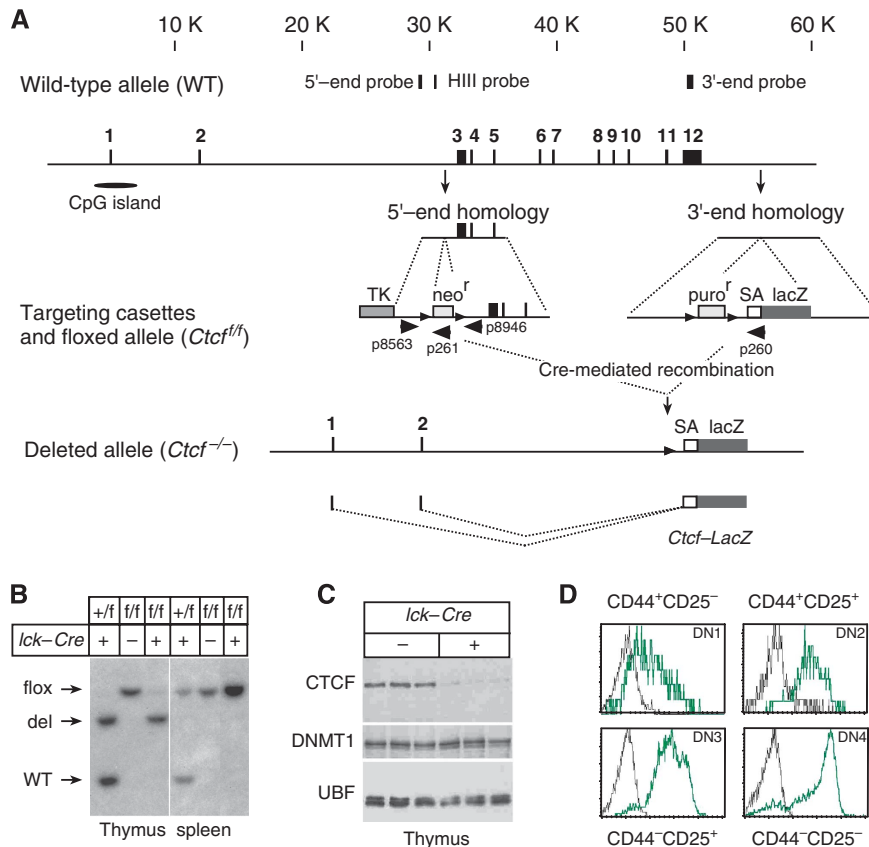


Figure 1 Conditional targeting of the mouse *Ctf* gene. (A) Murine *Ctf* locus and gene targeting constructs. Exons of the *Ctf* gene (solid boxes) are numbered, scale is in kilobase (K). Exon 1 is embedded in a CpG island. Exon 3 contains the start codon, and exon 12 contains the stop codon. Southern blot probes (5'-end and HIII) are shown above the *Ctf* gene. The two targeting constructs, with loxP sites (small triangles), flanking a PMC1-neomycin cassette (*neo*^f) or a PGK-puromycin cassette (*puro*^f), are shown with homologous regions. TK, thymidine kinase gene; SA-LacZ, Splice acceptor-lacZ cassette (Hoogenraad *et al*, 2002). PCR primers for genotyping (p8563, p8946, p260 and p261, large triangles) are indicated on targeting cassettes. Underneath the targeting constructs, the deleted *Ctf* gene is shown, which is generated after complete Cre-mediated recombination at the outermost loxP sites. Owing to alternative splicing, the splice acceptor (SA) site, present at the 5'-end of the reporter LacZ cassette, is spliced on to *Ctf* exon 1 or 2, thereby generating a hybrid *Ctf-lacZ* transcript. (B) Southern blot analysis of *Lck-Cre* recombinase activity. Digested genomic DNA from thymus and spleen of mice of the indicated genotypes was analysed by hybridization with the HIII probe (see panel A). The positions of the wild-type (WT), *Ctf*^{f/f} (flox) and *Ctf*^{-/-} (del) alleles are indicated. (C) Western blot analysis of thymus. Total thymus lysates from *Lck-Cre Ctf*^{f/f} and WT mice (+ indicates presence of Cre transgene; - indicates absence) were analysed for CTCF, DNMT1 and UBF protein levels. Three mice were analysed per genotype. (D) Flow cytometric analysis of lacZ expression in CTCF conditionally deleted mice. LacZ expression was analysed in conjunction with cell surface markers. The indicated cell populations were gated and lacZ expression data are displayed as histogram overlays of *Lck-Cre Ctf*^{f/f} mice (green) on top of background signals in wild-type mice (black).

Table I Genotype of *Ctf*^{+/-} × *Ctf*^{+/-} and *Ctf*^{+/-} × wild type offspring

Age	Genotype and number		
	Wild type	<i>Ctf</i> ^{+/-}	<i>Ctf</i> ^{-/-}
<i>Ctf</i> ^{+/-} × <i>Ctf</i> ^{+/-}			
E 9.5	13	14	0
E 3.5	10	7	0
Adult	88	92	0
<i>Ctf</i> ^{+/-} × wild type			
Adult	101	74	NA

increase in DN3, DN4 and ISP cells, is observed (Figure 2A and B, Table II). Thus, the effect of a complete *Ctf* knockout is particularly prominent at the ISP-to-DP transition (Figure 2B). The fact that the absolute number of *Ctf* knockout thymocytes increases about four-fold from ISP to DP, compared with a 90-fold increase in wild-type mice

(Figure 2C and Table II), suggests that a cell cycle block rather than increased apoptosis underlies the accumulation of ISP cells from *Lck-Cre Ctf*^{f/f} mice.

Heterozygous *Lck-Cre Ctf*^{+/-} mice also display a phenotype, which is most obvious at the DP stage (Figure 2B, Table II). In these mice, thymic cellularity is only modestly reduced and no accumulation of ISP cells is detected (Table II). These results show that normal CTCF levels are important for proper T-cell development. In agreement with impaired thymic SP cell production, the number of mature CD4⁺ and CD8⁺ T cells in spleen and lymph nodes of *Lck-Cre Ctf*^{f/f} and *Lck-Cre Ctf*^{+/-} mice are significantly reduced (Figure 2A, B; and H Heath, CR de Almeida, RW Hendriks and N Galjart, unpublished data). Interestingly, the ratio between mature CD4⁺ SP and DP cells, and between CD8⁺ SP and DP thymocytes, is similar in heterozygous *Lck-Cre Ctf*^{+/-}, homozygous *Lck-Cre Ctf*^{f/f} and wild-type mice (Figure 2C), indicating that differentiation from the DP to SP stage is not severely affected by a deletion of CTCF.

Table II Average numbers of thymocyte subpopulations derived from *Lck-Cre Cctf^{fl/fl}* mice (homozygous), *Lck-Cre Cctf^{+/fl}* mice (heterozygous) and wild-type (WT) mice

Genotype	DN1	DN2	DN3	DN4	ISP	DP	CD4 SP	CD8 SP	Total
WT (<i>n</i> = 14)	0.27 ± 0.02	0.37 ± 0.05	2.09 ± 0.19	1.10 ± 0.13	1.81 ± 0.21	165 ± 10.3	14.1 ± 1.08	5.56 ± 0.58	191 ± 11.7
Heterozygous (<i>n</i> = 7)	0.32 ± 0.03	0.66 ± 0.14	3.42 ± 0.93	0.73 ± 0.16	1.92 ± 0.31	95.9 ± 7.40	7.66 ± 0.81	2.48 ± 0.35	113 ± 8.77
Homozygous (<i>n</i> = 12)	0.39 ± 0.08	0.91 ± 0.26	4.72 ± 0.85	3.15 ± 0.40	9.14 ± 1.82	35.4 ± 1.89	2.19 ± 0.50	0.81 ± 0.20	56.7 ± 3.76
<i>P</i> -value (heterozygous-WT)	NS	NS	NS	NS	NS	<0.0001	0.0001	0.0002	<0.0001
<i>P</i> -value (homozygous-WT)	NS	NS	0.0082	0.0002	0.0014	<0.0001	<0.0001	<0.0001	<0.0001

NS, not significant.

Average values are given in millions of cells ± s.e.m.
P-values were calculated using a two-tailed student *t*-test.

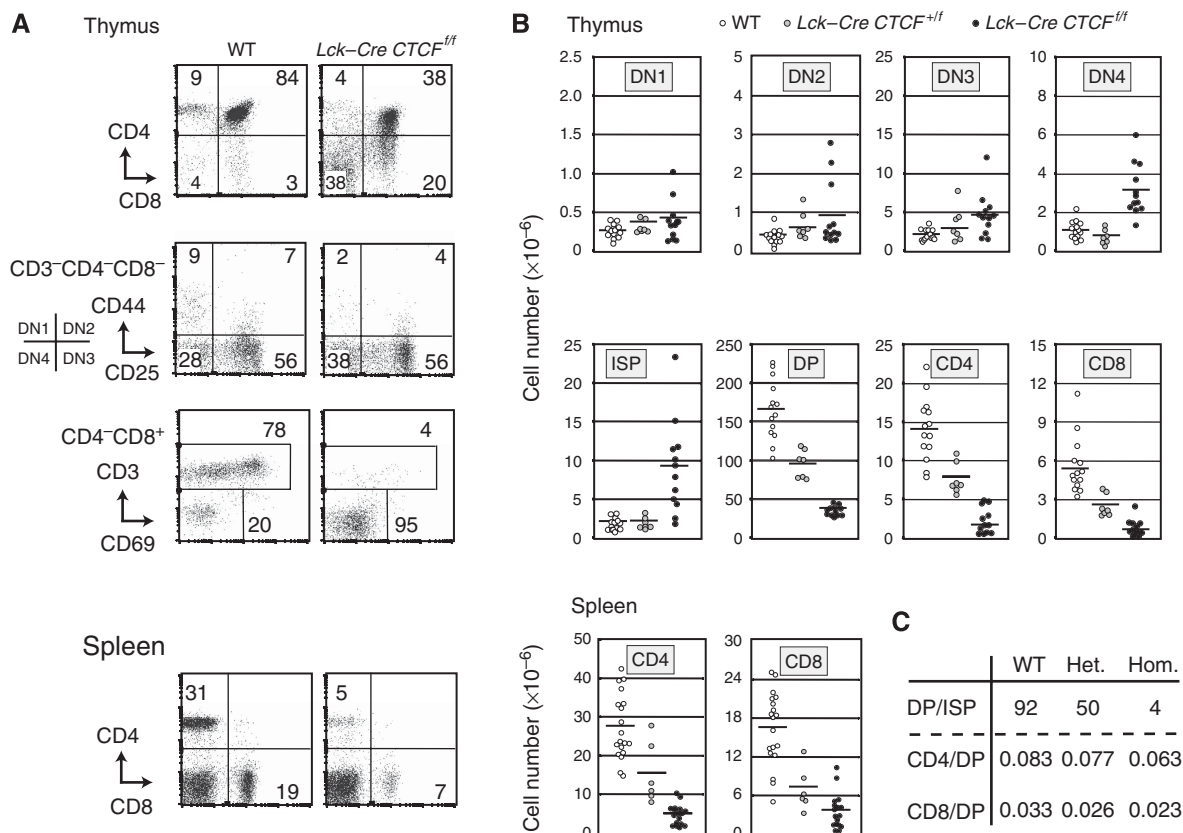


Figure 2 Defective TCR $\alpha\beta$ lineage development in CTCF-deficient mice. **(A)** Representative flow cytometric analyses of cell populations from thymus (upper three panels) and spleen (lower panel) derived from wild-type (WT) and *Lck-Cre Cctf^{fl/fl}* mice. Expression profiles of surface markers (indicated on the left) are shown as dot plots, and the percentages of cells within quadrants or gates are given. The DN1–DN4 cell populations (second panel from top) were gated on the basis of CD44 and/or CD25 expression, using the CD3[−]CD4[−]CD8[−] triple-negative fraction as a basis. The third panel from the top shows gating of the ISP and CD8 SP cell populations (on the basis of low and high expression of CD3, respectively) using the fraction of CD4[−]CD8⁺ thymocytes (indicated in the CD4/CD8 profile of the upper panel). Note the accumulation of ISP cells in the thymus of the *Lck-Cre Cctf^{fl/fl}* mouse (95%) compared with wild type (20%). **(B)** Number of thymic and splenic T cell subpopulations. Each symbol represents one individual animal (*n* = 12 for *Lck-Cre Cctf^{fl/fl}* mice, *n* = 7 for *Lck-Cre Cctf^{+/fl}* mice, and *n* = 14 for wild-type (WT) mice). Note that different scales are used in the vertical axes. Horizontal lines indicate average values (see Table II for actual values ± s.e.m.). *Lck-Cre Cctf^{fl/fl}* mice show increased numbers of DN3 (*P* < 0.01), DN4 (*P* = 0.0002) and ISP cells (*P* < 0.002) compared with wild type. In *Lck-Cre Cctf^{fl/fl}* mice and heterozygous *Lck-Cre Cctf^{+/fl}* mice DP, CD4 SP and CD8 SP subsets in the thymus were significantly reduced (*P* < 0.0001). CD4 and CD8 T cells in the spleen were significantly reduced in *Lck-Cre Cctf^{fl/fl}* mice (*P* < 0.00001) and in heterozygous *Lck-Cre Cctf^{+/fl}* mice (*P* < 0.01). **(C)** Analysis of cell numbers. Ratios were calculated (DP to ISP, CD4⁺ to DP, and CD8⁺ SP to DP) in *Lck-Cre Cctf^{fl/fl}* mice (hom), *Lck-Cre Cctf^{+/fl}* mice (het) and wild-type (WT) mice. The DP/ISP ratio indicates the fold increase in cells and correlates with number of cell divisions. By contrast, the CD4/DP and CD8/DP ratios show a decrease in cell number and are a measure of selection.

The accumulation of CTCF-deficient ISP cells in *Lck-Cre Cctf^{fl/fl}* mice could result from a developmental arrest at the ISP stage or alternatively reflect defective upregulation of CD4 expression in cells that otherwise have characteristics of DP cells, similar to thymocytes deficient for the chromatin remodeler Mi-2 β (Williams *et al*, 2004). To distinguish be-

tween these possibilities, we assessed expression of various cell surface markers in wild-type and *Lck-Cre Cctf^{fl/fl}* thymocytes. Normally, surface expression of TCR β and its associated signalling molecule CD3 are low in ISP cells and are induced at the DP stage. CTCF-deficient ISP cells express low levels of CD3 and TCR β (Figure 3A). Furthermore, wild-type

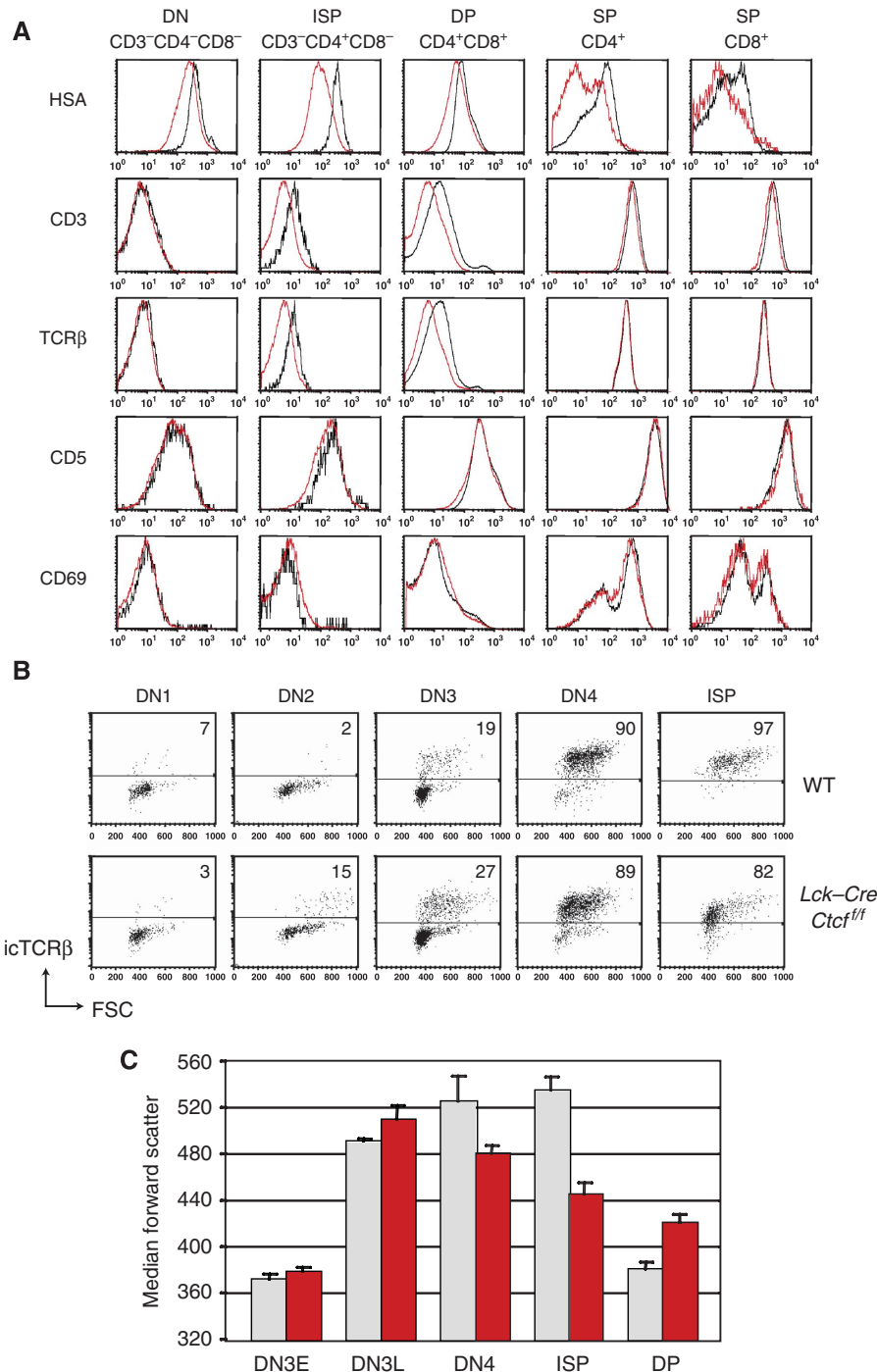


Figure 3 Characterization of CTCF-deleted thymocytes. **(A)** Expression of ISP cell markers. Flow cytometric analyses of HSA, CD3, TCR, CD5 and CD69 in thymocyte subpopulations, displayed as overlays of wild-type mice (black histograms) and *Lck-Cre Cctf^{1/1}* mice (red histograms). Data shown are representative of 5–8 mice per group. **(B)** Intracellular TCRβ levels in wild-type and *Lck-Cre Cctf^{1/1}* mice. Representative flow cytometric analyses of intracellular TCRβ protein expression in the indicated thymic subsets from a wild-type (WT) and an *Lck-Cre Cctf^{1/1}* mouse. TCRβ/forward scatter (FSC) profiles are shown as dot plots, gating is indicated by the horizontal lines and the percentages of TCRβ⁺ cells are shown. **(C)** Cell size in wild-type and *Lck-Cre Cctf^{1/1}* thymocytes. Quantification of median forward scatter values (which accurately reflects cell size) of the indicated thymocyte subpopulations in wild-type (grey bars) and *Lck-Cre Cctf^{1/1}* (red bars) mice. Data are average values ± s.e.m. from 5 to 8 mice per group.

and CTCF-negative ISP and DP cells express similar amounts of the surface glycoprotein CD5, which is normally upregulated on ISP cells and somewhat further on DP cells (Azzam *et al*, 1998). CTCF-deficient ISP cells also express low levels of CD69, which in wild-type mice is induced in a subfraction of DP cells, reflecting TCR-mediated activation (Bendelac *et al*,

1992). Expression of heat stable antigen (HSA, also called CD24, a cell adhesion molecule), which is normally high on DN and ISP cells and downregulated at the ISP-to-DP transition (Williams *et al*, 2004), is reduced in CTCF-deficient cells throughout thymocyte differentiation (Figure 3A). As none of the markers tested show a ‘DP-like’ expression pattern in

CD3-CD4⁻CD8⁺ cells in *Lck-Cre Cctf^{ff}* mice, we conclude that these accumulating cells truly represent ISP cells and not aberrant DP cells that fail to upregulate CD4 expression. In addition to the ISP-to-DP arrest in *Lck-Cre Cctf^{ff}* mice, we observed a significant increase in number of cells within the preceding DN3 and DN4 stages (Table II), indicating that a deletion of CTCF causes a developmental arrest from DN3 to ISP.

Interestingly, the expression level of CD3 is not only reduced in ISP thymocytes from *Lck-Cre Cctf^{ff}* mice, but also in DP cells and—to a lesser extent—in mature CD4⁺ SP and CD8⁺ SP cells (Supplementary Figure S3A, note that in CD8 SP cells, the decrease is not significant). In particular, CTCF-deficient DP cells do not contain the fraction of CD3^{high}/TCR^{high} cells. DP cells from heterozygous *Lck-Cre Cctf^{+/ff}* mice express CD3 levels that are in the range of those from WT mice (Supplementary Figure S3A), showing that only a complete lack of CTCF affects CD3 expression at the DP cell stage. Although CTCF-negative DP thymocytes are affected in the expression of important molecular markers, including CD3 and TCR, they are still able to differentiate towards the mature SP stages.

Defective cell-size regulation in the TCR $\alpha\beta$ lineage in *Lck-Cre Cctf^{ff}* mice

As our findings indicated a specific function of CTCF at the ISP-to-DP transition, we focussed our attention on possible mechanisms underlying the hampered differentiation of these cells. We first analysed *Tcr* rearrangement, because of the many CTCF-binding sites that are found in the genes encoding the different receptors. *Tcr β* gene rearrangement is generally initiated and completed in DN3. This stage consists of early small DN3E cells that have not yet productively rearranged the *Tcr β* locus, and more mature large proliferating DN3L cells expressing TCR β (Hoffman *et al*, 1996). We detect a significant increase in the population of large DN2 cells in *Lck-Cre Cctf^{ff}* mice that contain intracellular TCR β ⁺ (Figure 3B, 13 ± 4% in CTCF-deficient DN2 cells ($n = 3$), compared with 4 ± 0.5% in wild-type controls ($n = 4$); $P < 0.01$). These results raise the interesting possibility that CTCF is involved in inhibiting recombination early in development. The proportion of large TCR β ⁺ DN3 cells appears still elevated, but the difference between the two groups (~21 and ~18% in CTCF-deficient and wild-type mice, respectively) is not significant. Thus, the *Tcr β* locus can undergo functional V(D)J recombination in cells that have deleted the *Cctf* gene. It should be noted that even though the *Cctf* gene is efficiently deleted using the *Lck-Cre* transgene, residual CTCF protein might still be present at DN2 and DN3 stages, and we cannot rule out that this is sufficient for recombination.

By comparing wild-type and *Lck-Cre Cctf^{ff}* mice, we found that CTCF-negative TCR β ⁺ DN3 cells have the capacity to increase their cell size at the developmental progression of TCR β ⁻ DN3E to TCR β ⁺ DN3L cells (Figure 3B and C). However, from the DN3L-to-ISP stage, CTCF-deficient cells become much smaller than wild-type cells (Figure 3B and C). CTCF-deficient DP cells are again larger than wild-type cells (Figure 3C, Supplementary Figure S3B) and continue to be larger throughout subsequent differentiation (Supplementary Figure S3B). These results indicate that CTCF is a critical regulator of cell growth of $\alpha\beta$ T cells. Cells from heterozygous

Lck-Cre Cctf^{+/ff} mice are sized like wild types (Supplementary Figure S3A), showing that only a complete lack of CTCF affects cell size.

Developmental arrest of CTCF-deficient thymocytes is not due to defective *Tcr* rearrangements

The severe reduction of DP cell numbers and low-surface CD3/TCR expression on CTCF-deficient DP cells, together with the reported presence of CTCF-binding sites in the *Tcr α* gene locus (Garrett *et al*, 2005; Kim *et al*, 2007), indicated that defective TCR α V(D)J recombination could contribute to the arrest of CTCF-deficient thymocytes. We therefore crossed *Lck-Cre Cctf^{ff}* mice with transgenic mice expressing either the pre-rearranged OTII TCR $\alpha\beta$, which recognizes the OVA_{323–339} peptide in the context of C57BL/6 MHC class II, and which positively selects thymocytes towards the CD4 lineage (Barnden *et al*, 1998), or the MHC class I-restricted HY TCR $\alpha\beta$, which recognizes a male-specific HY antigen peptide in the C57BL/6 H-2^b class I female background and normally drives thymocytes into the CD8 lineage (Kisielow *et al*, 1988). However, the impaired developmental progression of CTCF-deficient cells is not rescued (Figure 4). Rather, the presence of the OTII and HY TCR transgenes results in an even more severe arrest of T-cell development in the thymus (Figure 4A and B, respectively). OTII Tg *Lck-Cre Cctf^{ff}* mice manifest a relative increase in the proportions of DN and ISP cells in the thymus, whereas the proportions of DP and CD4 SP cells are reduced. In addition, we observe an almost complete absence of mature T cells in the spleen (Figure 4A). HY Tg *Lck-Cre Cctf^{ff}* mice manifest a severe block at the ISP stage and an almost complete lack of DP cells in the thymus. Those CD8⁺ cells present in CTCF-deficient HY Tg mice are ISP cells rather than mature CD8 SP cells, because the level of HY-specific TCR expression (as detected by the T3.7 antibody) in the CD8⁺ cell fraction is substantially lower, when compared with wild-type CD8 SP cells. In agreement with this, CD4 or CD8 cells in the spleen are strongly reduced (Figure 4B). Thus, providing *Lck-Cre Cctf^{ff}* mice with a pre-rearranged TCR $\alpha\beta$ does not correct the developmental arrest of DP cells, indicating that the developmental block in *Cctf* knockout T cells is independent of *Tcr* gene rearrangement.

We next crossed *Lck-Cre Cctf^{ff}* mice with mice deficient for the *Recombination activating gene 2* (*Rag2*) gene. RAG2 mediates V(D)J recombination of *Tcr* and *Ig* loci. *Rag2^{-/-}* mice are therefore deficient in *Tcr* gene rearrangement, and they normally do not progress beyond the DN3 stage (Figure 5). *In vivo* stimulation with anti-CD3 ϵ antibodies mimics pre-TCR signalling (Azzam *et al*, 1998) and thereby induces the formation of DP cells in the absence of rearrangement. Both in *Rag2^{-/-}* and in CTCF-deficient *Rag2^{-/-}* mice, we find that on anti-CD3 ϵ treatment, total thymic cellularity increases from $< 2 \times 10^6$ to 13 ± 4 and $11 \pm 3 \times 10^6$, respectively ($n = 4$ in each group) and equal numbers of DN4 cells are induced (Figure 5). However, the formation of DP cells is reduced in CTCF-deficient *Rag2^{-/-}* mice, when compared with CTCF-expressing cells (Figure 5).

As the *Tcr γ* and δ loci can also undergo functional V(D)J recombination in the absence of CTCF, we conclude that the multiple CTCF-binding sites reported to be present in *Tcr* loci (Magdinier *et al*, 2004; Garrett *et al*, 2005; Barski *et al*, 2007) do not appear to be essential for the process of V(D)J

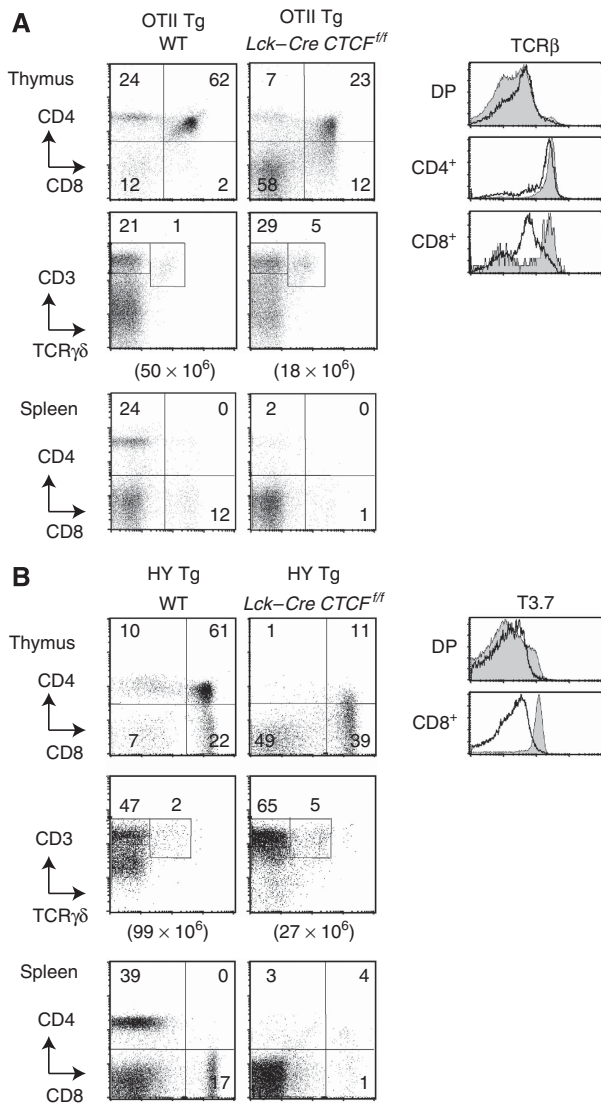


Figure 4 Arrest of CTCF-deficient thymocytes remains despite *Tcr* gene rearrangement. (A) Representative flow cytometric analyses of cell populations from thymus (upper two panels) and spleen (lower panel) derived from OTII transgenic mice, which are either in a wild-type (WT) or in a *Lck-Cre Ctcf^{f/f}* background. Expression profiles of CD4/CD8 and CD3/TCR $\gamma\delta$ markers are shown as dot plots; and the percentages of cells within quadrants or gates are given. Thymic cellularity is shown for the individual animals underneath the second panel. In the right hand panels, data for the OTII transgenics are displayed as histogram overlays. The expression profile of total surface TCR β within the indicated cell populations is shown for *Lck-Cre Ctcf^{f/f}* mice (bold lines) on top of profiles of WT littermates (grey-filled histograms). (B) Representative flow cytometric analyses of cell populations from thymus (upper two panels) and spleen (lower panel) derived from HY transgenic mice, which are either in a wild-type (WT) or in a *Lck-Cre Ctcf^{f/f}* background. Flow cytometric profiles of CD4/CD8 and CD3/TCR $\gamma\delta$ are shown as dot plots; percentages of cells within quadrants or regions and total thymic cell numbers are given. The expression profile of total HY idiotype-specific T3.7 TCR within the indicated cell populations is shown on the right as a histogram overlay of *Lck-Cre Ctcf^{f/f}* mice (bold lines) on top of profiles of WT littermates (grey-filled histograms).

recombination. Therefore, deficiency of CTCF results in a developmental block at the ISP-to-DP transition that is independent of *Tcr* gene rearrangement.

Cell cycle arrest during TCR $\alpha\beta$ lineage development in *Lck-Cre Ctcf^{f/f}* mice

To further examine the underlying cause of the accumulation of CTCF-negative ISP cells, we sorted wild-type and CTCF-deleted cells T cells into DN, ISP and DP fractions, and used real-time PCR to analyse mRNA expression patterns of a selected number of important T-cell factors. In wild-type cells, *Ctcf* mRNA levels increase from the DN-to-ISP stage and then decrease again in DP cells (Figure 6A). These data suggest that the relatively large, actively cycling ISP cells require a higher amount of CTCF for normal functioning than DN or DP cells. In sorted cells from *Lck-Cre Ctcf^{f/f}* mice, *Ctcf* expression is severely reduced in the DN fraction and is absent at later stages (Figure 6A; note that residual *Ctcf* mRNA is detected in the DN pool because the *Ctcf* gene is only fully deleted from DN2 onwards).

CTCF was reported to be a negative transcriptional regulator of *c-Myc* (Lobanenkov *et al*, 1990; Qi *et al*, 2003), and *c-Myc* is important for T-cell development (Trumpp *et al*, 2001). In wild-type T cells, *c-Myc* is expressed in a pattern different from *Ctcf* (Figure 6A). In addition, *c-Myc* expression is hardly affected by a CTCF deletion. Therefore, in T cells, CTCF does not appear to regulate expression of the *c-Myc* gene. The level of DNMT1, a maintenance methyltransferase that is essential for T-cell development (Lee *et al*, 2001), is also similar in wild-type and CTCF-deleted T cells (Figure 6A, see also Figure 1C). Two other transcription factors are GATA3, which is critically involved in β -selection and development of CD4 SP cells (Pai *et al*, 2003), and SATB1, which organizes cell type-specific nuclear architecture (Cai *et al*, 2006). In wild-type cells, the levels of these factors are opposite to those of *Ctcf* (Figure 6A). In CTCF-deficient cells, *Gata3* and *Satb1* expression is reduced, in particular at the DP stage. We next tested two cytoplasmic factors involved in T-cell signalling. Expression of PreT α (that assembles with TCR β to initiate TCR signalling) is not affected in ISP cells and is up-rather than downregulated in DP cells in the absence of CTCF (Figure 6A). Finally, the expression of GIMAP4, which is induced by pre-TCR signalling and accelerates T-cell death (Schnell *et al*, 2006), is increased in CTCF-deficient DP T cells with a factor of ~ 2 (Figure 6A). Nevertheless, we did not find evidence for increased apoptosis of CTCF-deficient DP cells (data not shown). Although none of the factors tested appears to be directly regulated by CTCF, changes in their expression level may contribute to the observed phenotype in CTCF-deleted cells.

As the accumulation of ISP cells from *Lck-Cre Ctcf^{f/f}* mice could be due to cell cycle defects, we tested the expression of two major cell cycle inhibitors, *p21* and *p27*. In wild-type cells, the expression profile of these factors is opposite to that of *Ctcf*, whereas *Ctcf* knockout cells show significantly increased *p21* and *p27* expression (Figure 6A). We subsequently analysed cell cycle profiles in wild-type and CTCF-deleted thymocytes. The CTCF-deficient ISP population from *Lck-Cre Ctcf^{f/f}* mice contains approximately half the number of cycling cells compared with wild type ($29\% \pm 1$ cells in S/G2/M phase in *Lck-Cre Ctcf^{f/f}* mice ($n = 3$), versus $53\% \pm 8$ in wild-type mice ($n = 3$); Figure 6B shows an example of analysis from individual mice). These results indicate that cell cycle progression in β -selected CTCF-deficient T cells is blocked due to the upregulation of *p21* and *p27*.

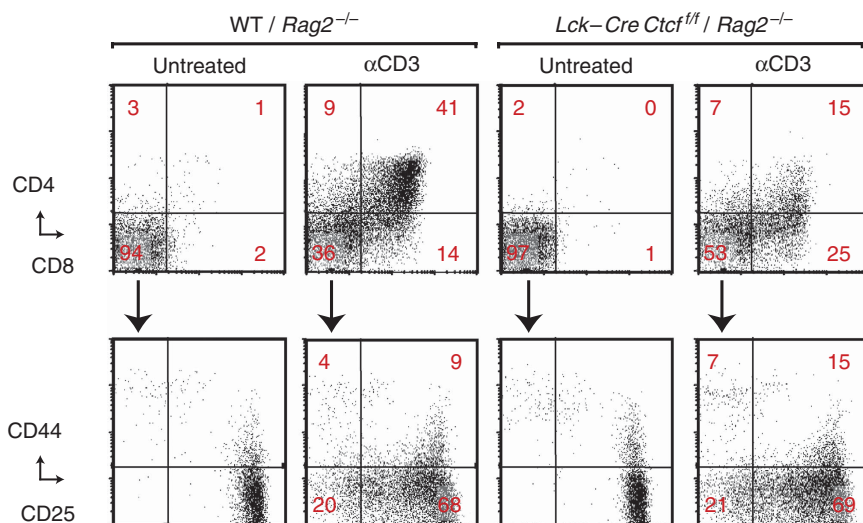


Figure 5 Arrest of CTCF-deficient thymocytes is independent of *Tcr α* gene rearrangement. Representative flow cytometric analyses of the thymus of *Rag2* knockout (*Rag2*^{-/-}) mice, which are either in a wild-type (WT) or in a *Lck-Cre Ctf*^{1/f} background. Mice were either untreated or injected with 50 μ g of rat anti-CD3 antibodies (α CD3) *in vivo*. The CD4 and CD8 expression profiles, 3 days after injection, are shown (upper part). Cell populations were gated (vertical and horizontal lines) and the CD4⁻CD8⁻ fraction (i.e., DN cells) was analysed for CD25 and CD44 expression (lower part). Data are shown as dot plots and the percentages of cells within the quadrants are given. The plots shown are representative for four mice in each group.

We next tested whether a deletion of CTCF always causes upregulation of the *p21* and *p27* genes, irrespective of cell type. We treated mouse embryonic fibroblasts (MEFs) from *Ctf*^{1/f} mice with Cre recombinase (Splinter *et al*, 2006) to efficiently remove CTCF in these cells. Real-time PCR experiments show that in MEFs the expression of *p21*, but not of *p27*, is increased in the absence of CTCF (Figure 6C). Thus, the combined upregulation of *p21* and *p27* seen in CTCF-deficient ISP cells is not a general regulatory mechanism.

CTCF as a critical regulator of cell growth and proliferation in $\alpha\beta$ T cells

Genome-wide studies in human cells have shown that CTCF-binding patterns in fibroblasts and T cells largely overlap (Barski *et al*, 2007; Kim *et al*, 2007). Interestingly, the human *p21* gene contains four CTCF binding sites in the vicinity of its promoter, whereas no binding sites are found near *p27*. As *p21* but not *p27* mRNA is upregulated in different cell types in the absence of CTCF, and CTCF binds near and within the human *p21* gene but not near *p27*, we hypothesized that CTCF might be a negative regulator of *p21* expression. This idea is enforced by the observation that in wild-type DN, ISP and DP thymocytes, the *p21* mRNA expression profile is exactly opposite to that of *Ctf* (Figure 6A). To test our assumption, we first confirmed that CTCF-binding sites (which are part of CNEs) are conserved between man and mouse. Chromatin immunoprecipitations (ChIPs) in MEFs on the corresponding regions of mouse *p21* indeed reveal an identical pattern of CTCF binding, including the two adjacent strong sites in intron 1 (Figure 6C).

Next, we analysed thymocytes isolated from total thymus and largely consisting of DP cells, and purified CD4⁺ T cells, either before (day 0) or after 3 days of *in vitro* activation by anti-CD3/anti-CD28 stimulation (day 3). We reasoned that in these cells, levels of *p21* must differ and that these cells therefore represent a good model to test whether CTCF binding correlates to *p21* expression in cells expressing

normal amounts of CTCF. We correlated mRNA expression levels of *Ctf* and *p21* (as tested with real-time PCR) with CTCF binding (as analysed by ChIP), using the strongest CTCF site in intron 1 of the *p21* gene as a reference. mRNA expression levels were normalized to *Hprt* (a housekeeping gene), whereas CTCF binding was normalized to the *Amylase* gene, which contains no CTCF-binding sites. The data show that CTCF binds very strongly to the *p21* intron, both in thymocytes and resting and cultured T cells (Figure 6D). Although there is a correlation between *Ctf* mRNA levels and strength of CTCF binding, there is no correlation with *p21* expression (Figure 6D). Thus, despite the fact that deletion of CTCF results in increased expression of *p21* in thymocytes and MEFs, the *p21* gene does not appear to be a general target of CTCF in wild-type cells.

The mRNA expression data indicate that *Ctf* is specifically upregulated in ISP cells (Figure 6A). Furthermore, lacZ staining results show increased activity of the *Ctf* promoter in DN2-DN4 cells (Figure 1D) and in ISP cells (not shown). However, both the PCR and LacZ staining results reflect mRNA levels of CTCF. To also analyse CTCF protein levels *in vivo*, we used a *Ctf*^{gfp} knock-in allele in which GFP-CTCF is expressed instead of CTCF (H Heath and N Galjart, unpublished data). We used flow cytometry to identify GFP-CTCF in the different thymocyte subsets and in the spleen (Supplementary Figure S4). During $\alpha\beta$ T-cell differentiation, CTCF levels increase from the DN2 to the ISP stage and then return to DN1 values in the DP cell population (Supplementary Figure S4A), consistent with the expression profile of *Ctf* transcripts (Figure 6A). In TCR $\alpha\beta$ CD4⁺ and CD8⁺ T cells in the spleen, CTCF levels are identical to the levels in DN1 and SP cells in the thymus (Supplementary Figure S4B). Thus, CTCF levels increase in those thymocyte populations (DN3, DN4 and ISP) that have a larger cell size (see Figure 3). Interestingly, a lack of CTCF causes accumulation of these very same cells. Taken together, our data suggest that CTCF is a critical regulator of cell growth and proliferation in $\alpha\beta$ T cells.

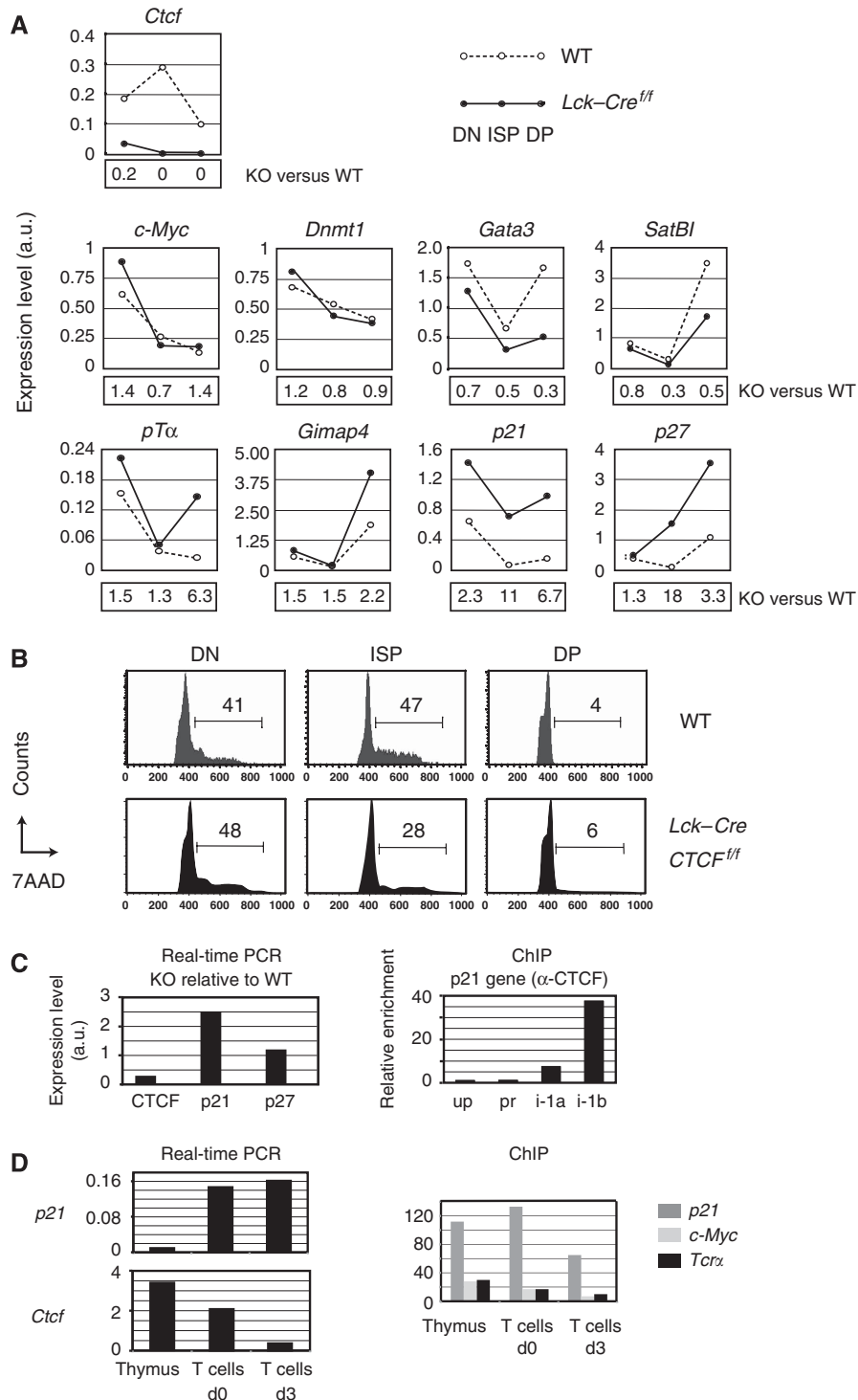


Figure 6 CTCF is important for cell cycle progression. **(A)** Quantitative RT-PCR analysis in sorted DN, ISP and DP cell fractions from wild-type (WT) and *Lck-Cre Ctf^{f/f}* mice. The DP fraction also contained CD4 SP cells. To obtain enough material, RNA was pooled from four WT and two *Lck-Cre Ctf^{f/f}* mice. **(B)** Cell cycle status of DN, ISP and DP cells isolated from WT and *Lck-Cre Ctf^{f/f}* mice. Cell cycle was analysed using 7-AAD, which measures DNA amount. A representative analysis is shown. Numbers indicate the percentage of cells in S/G2/M. In *Lck-Cre Ctf^{f/f}* mice, this number is significantly reduced in ISP cells, showing that this population is hampered in the cell cycle. **(C)** Quantitative RT-PCR (left hand panel) and ChIP (right hand panel) analysis in wild-type and *Ctcf^{f/f}* MEFs, after treatment with Cre recombinase. mRNA expression in Cre-treated *Ctcf^{f/f}* MEFs (KO) is shown relative to wild type. Although residual *Ctcf* mRNA is present in the MEFs, *p21* expression is increased. ChIP analysis was performed with anti-CTCF antibodies on four regions in the *p21* gene. Potential CTCF-binding sites in the mouse *p21* gene were chosen on the basis of a genome-wide analysis in human cells (Barski *et al*, 2007). An identical binding pattern was observed in wild-type MEFs, with relatively weak CTCF binding 2.3 kb upstream of the *p21* promoter (up) and on the promoter (pr), and very strong binding on two adjacent regions within intron 1 (i-1a, i-1b). **(D)** Quantitative RT-PCR (left hand panels) and ChIP (right hand panel) analysis in wild-type thymocytes and T cells before (d0) and after (d3) 3 days of anti-CD3/CD28 stimulation *in vitro*. mRNA expression of *p21* and *Ctcf* is shown relative to *Hprt*. ChIP analysis was performed with anti-CTCF antibodies on intron 1 of the *p21* gene and, as positive control, on known binding sites in the *c-Myc* and *Tcrα* genes.

Discussion

CTCF is an important protein involved in chromatin organization and the epigenetic regulation of gene expression. Most studies on CTCF use cultured cells as a basis, and a plethora of results regarding CTCF function have been reported. We have generated a conditional *Ctcf* knockout allele, which has allowed us to examine the *in vivo* function of CTCF. Consistent with a previous report (Fedoriw *et al*, 2004), we find that deletion of *Ctcf* in early embryonic development is lethal. A novel result is that heterozygous *Ctcf* knockout mice, which are viable and fertile, are born in less than expected numbers. The development of *Ctcf*^{+/-} thymocytes is also affected, although mildly. Taken together, these data suggest that CTCF is required in a dose-dependent manner.

We found no evidence for an increased tumour incidence in heterozygous *Ctcf* knockout animals, or for T lymphoid malignancies in CTCF-deficient T-cell lineages. This argues against a function of CTCF as a crucial tumour suppressor (Klenova *et al*, 2002). Increased expression of *p21* (and *p27*) in CTCF-negative cells would explain why loss of CTCF does not induce tumours. Still, the potential function of CTCF in cancer merits a more detailed investigation. We also do not observe a more severe phenotype in CTCF-deficient female thymocytes compared with male cells, suggesting that absence of CTCF does not cause deregulated expression of genes on the inactive X-chromosome. Moreover, the deletion of CTCF does not have an effect on the maintenance of methylation in the imprint control region of the *Igf2/H19* and ribosomal DNA (rDNA) loci (see Supplementary data). Unlike other studies (Schoenherr *et al*, 2003; Filippova *et al*, 2005), our results therefore indicate that CTCF is not required to maintain X-inactivation and DNA methylation status of the *Igf2/H19* locus.

Despite the presence of multiple CTCF-binding sites near the *Tcr α* and *Tcr β* genes, our data indicate that CTCF is not essential for recombination at these loci. CTCF also does not appear to be required for the differentiation of DP cells towards the CD4⁺ and CD8⁺ SP cell stage, even though substantial epigenetic and regulatory changes accompany commitment of SP cells (Rothenberg and Taghon, 2005). CTCF is, however, essential for the efficient proliferation of β -selected cells, in particular for their maturation from ISP to DP cells, and for TCR upregulation at the cell surface of DP cells. As T cells were directly isolated from mice, our data provide the first *in vivo* evidence for an important function of CTCF in cell cycle progression. In line with a proliferative block, we detect strongly increased expression of two major cell cycle inhibitors, *p21* and *p27*.

Our results in T cells are completely opposite to those obtained in WEHI 231 B lymphoma cells, where conditional expression of CTCF resulted in the up- rather than the down-regulation of *p21* and *p27*, whereas reduction of CTCF levels decreased rather than increased the expression of *p21* and *p27* (Qi *et al*, 2003). This could be due to the fact that the properties of the ISP thymocytes and WEHI 231 B cells are entirely different. ISP thymocytes are highly proliferating as a result of pre-TCR stimulation, whereas crosslinking of the B-cell receptor on WEHI 231 immature B cells results in cell-cycle arrest and apoptosis (thereby providing a model for self-tolerance by clonal deletion). This suggests that CTCF function is context dependent, although it should be noted that

our data were obtained *in vivo*, whereas the data in the WEHI 231 B lymphoma cells were obtained with stably transfected clones selected for high expression of CTCF sense or antisense mRNA (Qi *et al*, 2003). Using our conditional *Ctcf*^{fl/fl} mice in combination with existing B cell-specific Cre transgenes, we will be able to examine the function of CTCF in B cells.

In *Ctcf* knockout mice, approximately four times more DP cells are present than ISP cells, suggesting that the latter cells can divide, although slowly. Moreover, whereas CTCF-negative ISP cells are smaller than their wild-type counterparts, DP cells are larger. These data argue against increased apoptosis as a cause of reduction in DP cell numbers after *Ctcf* gene deletion. This is different from the situation in *Dnmt1* knockout mice, which have similar numbers of DN thymocyte subsets as wild-type littermates, and in which increased apoptosis was shown to be a major cause of the severe reduction in DP cell number (Lee *et al*, 2001).

T-cell activation at the DN3 stage is accompanied by an enlargement of both cytoplasmic and nuclear volume. In the DN4 and ISP stages, growth is coupled to proliferation, presumably to sustain the rapid cell divisions that are required in these cells. When thymocytes enter the DP stage, they exit the cell cycle and become small again. CTCF levels increase when cells become bigger (from DN3 to ISP) and decrease again when cells become small. Furthermore, CTCF-negative DN4 and ISP cells are smaller than wild-type cells, whereas DP cells are larger. These data uncover a function of CTCF as a regulator of cell growth and proliferation in thymocytes. A notable enrichment of CTCF-binding sites was observed near DNase I HSs in CD4⁺ T cells, indicating that CTCF controls global T-cell expression (Boyle *et al*, 2008). Our data suggest that CTCF couples cell growth to the cell cycle. Strikingly, the ratio between DP cell number and mature CD4⁺ SP and CD8⁺ SP thymocytes is the same in wild-type, heterozygous *Lck-Cre Ctcf*^{+/-} and homozygous *Lck-Cre Ctcf*^{fl/fl} mice. Thus, the major function of CTCF in the thymus might be to positively regulate cell growth in rapidly dividing thymocytes so that appropriate numbers of cells are generated before positive and negative selection events at the DP stage in the thymus.

Materials and methods

Modified *Ctcf* alleles, mouse models and embryonic fibroblasts

Human CTCF cDNA was used to screen a 129S6/SvevTac mouse PAC library (RPC1-21) (Osoegawa *et al*, 2000). PAC clones were used to isolate 6.7 kb (for 5'-end targeting) and 8 kb (for 3'-end targeting) *EcoRI* subclones. For 5'-end targeting, the 6.7 kb *EcoRI* fragment was used to amplify 1360 bp of 5'-end homology and 5340 bp of 3'-end homology. The homologous arms were cloned into a vector containing the neomycin resistance gene flanked by loxP sites (Hoogenraad *et al*, 2002). A viral thymidine kinase gene was inserted afterwards. For 3'-end targeting, we generated a *SpeI-EcoRI* subclone from the PAC DNA and used its unique *BamHI* site to insert a cassette containing the puromycin resistance gene flanked by loxP sites, followed by splice acceptor sequences and the bacterial β -galactosidase (*lacZ*) reporter (Hoogenraad *et al*, 2002). Relevant parts of the different constructs were verified by DNA sequencing.

Constructs were targeted into E14 embryonic stem (ES) cells as described (Hoogenraad *et al*, 2002). DNA from resistant ES cells was analysed with external radiolabelled probes by Southern blotting. Confirmation of homologous recombination was performed using different 5'-end and 3'-end probes (Figure 1A and B) and a PCR-based assay for genotyping. *Ctcf*^{fl/fl} mice were crossed

back more than 10 times to the C57BL/6 background. MEFs were isolated from *Ctcf^{fl/fl}* mice using published procedures (Akhmanova *et al*, 2005). Fibroblasts were treated with lentiviral Cre as described (Splinter *et al*, 2006).

Ctcf^{fl/fl} mice were bred to mice expressing chicken β -actin-Cre generating *Ctcf^{+/-}* animals. T-cell-specific deletion of *Ctcf* was achieved by breeding to *Lck-Cre* mice (Lee *et al*, 2001), which were kindly provided by Dr C Wilson (University of Washington, Seattle, WA, USA). Cre-specific primers were used for genotyping. In experiments where *Ctcf* knockout mice are compared with 'wild type' animals, the latter are littermates of the *Lck-Cre Ctcf^{fl/fl}* animals, that is, mice that express normal ('wild type') levels of CTCF. Thus, the 'wild type' mice may be truly wild type; they may contain the *Lck-Cre* transgene or the *Ctcf^{fl/fl}* allele, but never a combination of the latter two alleles.

HY/Rag2^{-/-} (C57BL/10) mice were purchased from Taconic Europe A/S (Denmark). OT-II mice have been described (Barnden *et al*, 1998). Mice were bred and maintained in the Erasmus MC animal care facility under specific pathogen-free conditions and analysed at 6–10 weeks of age. For anti-CD3 treatment, Rag2-deficient mice (Shinkai *et al*, 1992) were injected i.p. with 50 μ g of rat anti-CD3 antibodies (α CD3; clone 145-2C11) as described (Levitt *et al*, 1995). Experimental procedures were reviewed and approved by the Erasmus University committee of animal experiments.

DNA, RNA and protein analysis

Genomic DNA was isolated, digested and blotted onto Hybond N+ membranes (Amersham) and hybridized with radiolabelled probes. *Ctcf* probes are shown in Figure 1. Total RNA was prepared using RNA-Bee RNA isolation solvent (Tel-Test Inc.). RNA (0.5–1.0 μ g) was reverse-transcribed (RT) with random and oligo-dT primers, in the presence of Superscript reverse transcriptase (Invitrogen). For the experiment shown in Figure 6, RNA was isolated and pooled from the thymus of four wild-type mice and from two *Lck-Cre Ctcf^{fl/fl}* mice.

Real-time RT-PCR was performed as described (Splinter *et al*, 2006) with 100 ng of each primer and 0.5 U of Platinum *Taq* DNA polymerase (Invitrogen). Sybr-green (Sigma) was added to the reactions and PCR was performed on a DNA Engine Opticon PCR system (MJ Research Inc.) and Bio-Rad MyiQ iCycler single-colour real-time PCR detection system. To confirm the specificity of the amplification products, samples were separated by standard agarose gel electrophoresis. Threshold levels were set and further analysis was performed using the SDS v1.9 software (Applied Biosystems). The obtained C_t values were normalized to the C_t value of *Gapdh*, β -actin or *Hprt*. Each PCR was performed at least in triplicate, and at least two independent experiments were performed to examine the expression of individual genes. Primer sequences and PCR conditions used are available on request.

For ChIP, nuclear extracts were prepared (Splinter *et al*, 2006). Chromatin cross-linking (2 \times 10⁷ cells treated with 1% formaldehyde for 10 min at room temperature), sonication to 300–800 base pair fragments and immunoprecipitation were as described (Upstate protocol, <http://www.upstate.com>). At least two independent ChIPs were carried out per experiment. Quantitative real-time PCR was performed as described above. Values were normalized to input measurements and enrichment was calculated relative to the

Amylase gene using the comparative C_t method. PCR products were all smaller than 150 bp. Primer sequences and PCR conditions used are available on request.

Western blot analysis was performed as described (Hoogenraad *et al*, 2002). Primary antibody incubation was done overnight at 4°C in Tris-buffered saline, containing 5% (w/v) BSA and 0.15% (v/v) NP-40. Blots were incubated with secondary goat anti-rabbit or anti-mouse antibodies, coupled to horseradish peroxidase (GE Healthcare UK Ltd: 1:50 000). Signal detection was performed using ECL (Amersham). Anti-CTCF (N3) and anti-fibrillarin (no. 4118 and 4080) antibodies were generated as described (Hoogenraad *et al*, 2000) using GST-linked chicken CTCF (amino acids 2–267) and fibrillarin fusion proteins. These antisera were used in a 1:300 dilution. DNMT1 (Abcam), and UBF (Santa Cruz Biotechnology) mAbs were used at 1:100. Western blots were scanned and the levels of protein were quantified using the gel macro function in ImageJ (Rasband, WS, NIH, <http://rsb.info.nih.gov/ij/>). The amount of CTCF was normalized to DNMT1 in the same sample.

Flow cytometric analyses

Preparation of single-cell suspensions, FDG-loading, mAb incubations for four-color cytometry have been described (Hendriks *et al*, 1996). All mAbs were purchased from BD Biosciences (San Diego, CA). Samples were acquired on a FACSCaliburTM flow cytometer and data was analysed using CellQuestTM software (BD Bioscience). For cell cycle profiles of thymic subsets, cells were first stained for surface markers, fixed with 0.25% paraformaldehyde and permeabilized with 0.2% Tween 20. Next, 7-AAD was added to a final concentration of 15 μ g/ml in PBS. Cell cycle status of T-cell cultures was determined after fixing in ice-cold ethanol and subsequent staining in PBS, containing 0.02 mg/ml propidium iodide, 0.1% v/v Triton X-100 and 0.2 mg/ml RNase. Doublet cells were excluded by measuring peak area and width. FACS sorting of DN, ISP and DP cells was performed with a FACS Vantage VE equipped with Diva Option and BD FACSdiva software (BD bioscience). The purity of fractions was >98%.

Statistical analysis

Statistical evaluations were performed by standard two-tailed *t*-test.

Supplementary data

Supplementary data are available at *The EMBO Journal* Online (<http://www.embojournal.org>).

Acknowledgements

We thank Dr C Wilson (University of Washington, Seattle, WA, USA) for providing us with *Lck-Cre* transgenic mice, and An Langeveld, Harmjan Kuiper, Janneke Samsom, Lisette van Berkel, Edwin de Haas, Tom Schoonerwille, Marjolein de Bruin and Jan Piet van Hamburg for their assistance. This work was supported by the Dutch Cancer Society (KWF), the European Science Foundation EUROCORES Programme EuroDYNA (ERAS-CT-2003-980409), Fundação para a Ciência e a Tecnologia and the Association for International Cancer Research (AICR).

References

- Akhmanova A, Matusset-Bonnefont AL, van Cappellen W, Keijzer N, Hoogenraad CC, Stepanova T, Drabek K, van der Wees J, Mommaas M, Onderwater J, van der Meulen H, Tanenbaum ME, Medema RH, Hoogerbrugge J, Vreeburg J, Uringa EJ, Grootegoed JA, Grosveld F, Galjart N (2005) The microtubule plus-end-tracking protein CLIP-170 associates with the spermatid manchette and is essential for spermatogenesis. *Genes Dev* **19**: 2501–2515
- Azzam HS, Grinberg A, Lui K, Shen H, Shores EW, Love PE (1998) CD5 expression is developmentally regulated by T cell receptor (TCR) signals and TCR avidity. *J Exp Med* **188**: 2301–2311
- Barnden MJ, Allison J, Heath WR, Carbone FR (1998) Defective TCR expression in transgenic mice constructed using cDNA-based alpha- and beta-chain genes under the control of heterologous regulatory elements. *Immunol Cell Biol* **76**: 34–40
- Barski A, Cuddapah S, Cui K, Roh TY, Schones DE, Wang Z, Wei G, Chepelev I, Zhao K (2007) High-resolution profiling of histone methylations in the human genome. *Cell* **129**: 823–837
- Bell AC, Felsenfeld G (2000) Methylation of a CTCF-dependent boundary controls imprinted expression of the *Igf2* gene. *Nature* **405**: 482–485
- Bell AC, West AG, Felsenfeld G (1999) The protein CTCF is required for the enhancer blocking activity of vertebrate insulators. *Cell* **98**: 387–396
- Bendelac A, Matzinger P, Seder RA, Paul WE, Schwartz RH (1992) Activation events during thymic selection. *J Exp Med* **175**: 731–742
- Boyle AP, Davis S, Shulha HP, Meltzer P, Margulies EH, Weng Z, Furey TS, Crawford GE (2008) High-resolution mapping and characterization of open chromatin across the genome. *Cell* **132**: 311–322

- Burke LJ, Zhang R, Bartkuhn M, Tiwari VK, Tavosoidana G, Kurukuti S, Weth C, Leers J, Galjart N, Ohlsson R, Renkawitz R (2005) CTCF binding and higher order chromatin structure of the H19 locus are maintained in mitotic chromatin. *EMBO J* **24**: 3291–3300
- Cai S, Lee CC, Kohwi-Shigematsu T (2006) SATB1 packages densely looped, transcriptionally active chromatin for coordinated expression of cytokine genes. *Nat Genet* **38**: 1278–1288
- Chien YH, Konigshofer Y (2007) Antigen recognition by gammadelta T cells. *Immunol Rev* **215**: 46–58
- Cobb BS, Hertweck A, Smith J, O'Connor E, Graf D, Cook T, Smale ST, Sakaguchi S, Livesey FJ, Fisher AG, Merckenschlager M (2006) A role for Dicer in immune regulation. *J Exp Med* **203**: 2519–2527
- Fedoriv AM, Stein P, Svoboda P, Schultz RM, Bartolomei MS (2004) Transgenic RNAi reveals essential function for CTCF in H19 gene imprinting. *Science* **303**: 238–240
- Filippova GN, Cheng MK, Moore JM, Truong JP, Hu YJ, Nguyen DK, Tsuchiya KD, Distchele CM (2005) Boundaries between chromosomal domains of X inactivation and escape bind CTCF and lack CpG methylation during early development. *Dev Cell* **8**: 31–42
- Filippova GN, Thienes CP, Penn BH, Cho DH, Hu YJ, Moore JM, Klesert TR, Lobanenko VV, Tapscott SJ (2001) CTCF-binding sites flank CTG/CAG repeats and form a methylation-sensitive insulator at the DM1 locus. *Nat Genet* **28**: 335–343
- Garrett FE, Emelyanov AV, Sepulveda MA, Flanagan P, Volpi S, Li F, Loukinov D, Eckhardt LA, Lobanenko VV, Birshtein BK (2005) Chromatin architecture near a potential 3' end of the igh locus involves modular regulation of histone modifications during B-Cell development and *in vivo* occupancy at CTCF sites. *Mol Cell Biol* **25**: 1511–1525
- Hark AT, Schoenherr CJ, Katz DJ, Ingram RS, Levorse JM, Tilghman SM (2000) CTCF mediates methylation-sensitive enhancer-blocking activity at the H19/Igf2 locus. *Nature* **405**: 486–489
- Hendriks RW, de Bruijn MF, Maas A, Dingjan GM, Karis A, Grosveld F (1996) Inactivation of Btk by insertion of lacZ reveals defects in B cell development only past the pre-B cell stage. *EMBO J* **15**: 4862–4872
- Hoffman ES, Passoni L, Crompton T, Leu TM, Schatz DG, Koff A, Owen MJ, Hayday AC (1996) Productive T-cell receptor beta-chain gene rearrangement: coincident regulation of cell cycle and clonality during development *in vivo*. *Genes Dev* **10**: 948–962
- Hoogenraad CC, Akhmanova A, Grosveld F, De Zeeuw CI, Galjart N (2000) Functional analysis of CLIP-115 and its binding to microtubules. *J Cell Sci* **113**: 2285–2297
- Hoogenraad CC, Koekoek B, Akhmanova A, Krugers H, Dortmund B, Miedema M, van Alphen A, Kistler WM, Jaegle M, Koutsourakis M, Van Camp N, Verhoye M, van der Linden A, Kaverina I, Grosveld F, De Zeeuw CI, Galjart N (2002) Targeted mutation of Cyln2 in the Williams syndrome critical region links CLIP-115 haploinsufficiency to neurodevelopmental abnormalities in mice. *Nat Genet* **32**: 116–127
- Kim TH, Abdullaev ZK, Smith AD, Ching KA, Loukinov DI, Green RD, Zhang MQ, Lobanenko VV, Ren B (2007) Analysis of the vertebrate insulator protein CTCF-binding sites in the human genome. *Cell* **128**: 1231–1245
- Kisielow P, Bluthmann H, Staerz UD, Steinmetz M, von Boehmer H (1988) Tolerance in T-cell-receptor transgenic mice involves deletion of nonmature CD4+8+ thymocytes. *Nature* **333**: 742–746
- Klenova EM, Morse III HC, Ohlsson R, Lobanenko VV (2002) The novel BORIS+CTCF gene family is uniquely involved in the epigenetics of normal biology and cancer. *Semin Cancer Biol* **12**: 399–414
- Lee PP, Fitzpatrick DR, Beard C, Jessup HK, Lehar S, Makar KW, Perez-Melgosa M, Sweetser MT, Schlissel MS, Nguyen S, Cherry SR, Tsai JH, Tucker SM, Weaver WM, Kelso A, Jaenisch R, Wilson CB (2001) A critical role for Dnmt1 and DNA methylation in T cell development, function, and survival. *Immunity* **15**: 763–774
- Levelt CN, Mombaerts P, Wang B, Kohler H, Tonegawa S, Eichmann K, Terhorst C (1995) Regulation of thymocyte development through CD3: functional dissociation between p56lck and CD3 sigma in early thymic selection. *Immunity* **3**: 215–222
- Lewis A, Murrell A (2004) Genomic imprinting: CTCF protects the boundaries. *Curr Biol* **14**: R284–R286
- Ling JQ, Li T, Hu JF, Vu TH, Chen HL, Qiu XW, Cherry AM, Hoffman AR (2006) CTCF mediates interchromosomal colocalization between Igf2/H19 and Wsb1/Nf1. *Science* **312**: 269–272
- Lobanenko VV, Nicolas RH, Adler VV, Paterson H, Klenova EM, Polotskaja AV, Goodwin GH (1990) A novel sequence-specific DNA binding protein which interacts with three regularly spaced direct repeats of the CCCTC-motif in the 5'-flanking sequence of the chicken c-myc gene. *Oncogene* **5**: 1743–1753
- Magdinier F, Yusufzai TM, Felsenfeld G (2004) Both CTCF-dependent and -independent insulators are found between the mouse T cell receptor alpha and Dad1 genes. *J Biol Chem* **279**: 25381–25389
- Ohlsson R, Renkawitz R, Lobanenko V (2001) CTCF is a uniquely versatile transcription regulator linked to epigenetics and disease. *Trends Genet* **17**: 520–527
- Osoegawa K, Tatenno M, Woon PY, Frengen E, Mammoser AG, Catanese JJ, Hayashizaki Y, de Jong PJ (2000) Bacterial artificial chromosome libraries for mouse sequencing and functional analysis. *Genome Res* **10**: 116–128
- Pai SY, Truitt ML, Ting CN, Leiden JM, Glimcher LH, Ho IC (2003) Critical roles for transcription factor GATA-3 in thymocyte development. *Immunity* **19**: 863–875
- Qi CF, Martensson A, Mattioli M, Dalla-Favera R, Lobanenko VV, Morse III HC (2003) CTCF functions as a critical regulator of cell-cycle arrest and death after ligation of the B cell receptor on immature B cells. *Proc Natl Acad Sci USA* **100**: 633–638
- Rothenberg EV, Tachon T (2005) Molecular genetics of T cell development. *Annu Rev Immunol* **23**: 601–649
- Sakai K, Miyazaki J (1997) A transgenic mouse line that retains Cre recombinase activity in mature oocytes irrespective of the cre transgene transmission. *Biochem Biophys Res Commun* **237**: 318–324
- Schnell S, Demolliere C, van den Berk P, Jacobs H (2006) Gimap4 accelerates T-cell death. *Blood* **108**: 591–599
- Schoenherr CJ, Levorse JM, Tilghman SM (2003) CTCF maintains differential methylation at the Igf2/H19 locus. *Nat Genet* **33**: 66–69
- Shinkai Y, Rathbun G, Lam KP, Oltz EM, Stewart V, Mendelsohn M, Charron J, Datta M, Young F, Stall AM, Alt FW (1992) RAG-2-deficient mice lack mature lymphocytes owing to inability to initiate V(D)J rearrangement. *Cell* **68**: 855–867
- Splinter E, Heath H, Kooren J, Palstra RJ, Klous P, Grosveld F, Galjart N, de Laat W (2006) CTCF mediates long-range chromatin looping and local histone modification in the beta-globin locus. *Genes Dev* **20**: 2349–2354
- Trumpp A, Refaeli Y, Oskarsson T, Gasser S, Murphy M, Martin GR, Bishop JM (2001) c-Myc regulates mammalian body size by controlling cell number but not cell size. *Nature* **414**: 768–773
- Williams CJ, Naito T, Arco PG, Seavitt JR, Cashman SM, De Souza B, Qi X, Keables P, Von Andrian UH, Georgopoulos K (2004) The chromatin remodeler Mi-2beta is required for CD4 expression and T cell development. *Immunity* **20**: 719–733
- Wolfer A, Wilson A, Nemir M, MacDonald HR, Radtke F (2002) Inactivation of Notch1 impairs VDJbeta rearrangement and allows pre-TCR-independent survival of early alpha beta lineage thymocytes. *Immunity* **16**: 869–879
- Xie X, Mikkelsen TS, Gnirke A, Lindblad-Toh K, Kellis M, Lander ES (2007) Systematic discovery of regulatory motifs in conserved regions of the human genome, including thousands of CTCF insulator sites. *Proc Natl Acad Sci USA* **104**: 7145–7150